

Manuscript version: Author's Accepted Manuscript

The version presented in WRAP is the author's accepted manuscript and may differ from the published version or Version of Record.

Persistent WRAP URL:

<http://wrap.warwick.ac.uk/151691>

How to cite:

Please refer to published version for the most recent bibliographic citation information. If a published version is known of, the repository item page linked to above, will contain details on accessing it.

Copyright and reuse:

The Warwick Research Archive Portal (WRAP) makes this work by researchers of the University of Warwick available open access under the following conditions.

© 2021 Elsevier. Licensed under the Creative Commons Attribution-NonCommercial-NoDerivatives 4.0 International <http://creativecommons.org/licenses/by-nc-nd/4.0/>.



Publisher's statement:

Please refer to the repository item page, publisher's statement section, for further information.

For more information, please contact the WRAP Team at: wrap@warwick.ac.uk.

Design resistance of helical seam pipe columns with limited tensile test data

Won-Hee Kang ^a, Stephen J. Hicks ^{b*}, Brian Uy ^c, Farhad Aslani ^{d,e}

^a Centre for Infrastructure Engineering, School of Engineering, Western Sydney University, Penrith, NSW 2751, Australia

^b School of Engineering, University of Warwick, Coventry, CV4 7AL, UK

^c School of Civil Engineering, The University of Sydney, Sydney, NSW 2006, Australia

^d Materials and Structures Innovation Group, School of Engineering, The University of Western Australia, Crawley, WA, 6009, Australia

^e School of Engineering, Edith Cowan University, Joondalup, WA, 6027, Australia

ABSTRACT

This study conducts a capacity factor calibration for steel and steel-concrete composite columns with helical seam pipe (also known as spiral welded tube) sections considering the following three member types: (i) steel columns under axial compression, (ii) concrete-filled steel tubes (CFSTs) under axial compression, and (iii) CFSTs under combined axial compression and uniaxial bending due to load eccentricity. The calibration has been conducted for both forward and inverse reliability analyses. The forward analysis calibrates the capacity factor of steel contribution in the design models given in NZS 3404.1, AS 4100, AS/NZS 5100.6 and AS/NZS 2327 to meet the target reliability level provided in both ISO 2394 and AS 5104 when using API 5L products in non-composite and composite column applications. Whilst the inverse analysis estimates the required minimum number of steel tensile tests when the target reliability level and the capacity factors are all provided. In these analyses, a total of 68 experimental data collected from the literature are utilised to estimate the modelling uncertainty in terms of bias and scatter. For all member types, the design models achieve similar or higher reliability than the target reliability, and the corresponding required minimum amount of steel material tests are calculated and provided.

26

27 *Keywords:* API 5L; steel-concrete composite columns; steel columns; design resistance; capacity
28 factors; steel reuse.

29

30 * Corresponding author.

31 E-mail address: Stephen.J.Hicks@warwick.ac.uk (S.J. Hicks).

32 **1. Introduction**

33 **1.1 Background**

34 Steel and concrete composite construction has achieved a high market share in multi-storey buildings
35 and bridges. Composite columns, or concrete-filled steel tubes (CFSTs), using circular hollow
36 sections have become popular because: greater resistance than rectangular or square hollow sections
37 is achieved through confinement of the concrete core [1,2,3]; the rules in current design standards
38 such as AS/NZS 2327 [4], EN 1994-1-1 [5], AISC 360-16 [6] imply that more structurally efficient
39 cross-sections can be achieved, due to reduced local buckling from the presence of the concrete infill
40 (however, it has recently been shown that this enhancement may be limited [7]); and improved
41 ductility and damping characteristics [8]. The presence of the steel section also eliminates the need
42 for formwork and, as the erection schedule is not dependent on concrete curing time in these situations,
43 CFSTs improve the speed of construction [9].

44 Whilst there has been a focus on the performance of CFSTs using standard section sizes, tailor-made
45 circular sections are becoming popular with designers as larger diameter (or non-standard diameter)
46 tubes can be specified in order that more structurally efficient solutions can be achieved. One of the
47 most popular types of tailor-made circular section are helical seam pipe, which are also known as
48 spiral welded tubes (SWTs). SWT's have historically been used in the conveyance of liquids or gases,

49 and are fabricated by helically bending a continuous length of steel plate and welding the abutting
50 edges [10]. The benefit of manufacturing SWTs compared to longitudinally welded tubes (LWTs)
51 arise from the efficiencies generated from the continuous spiral welding process, the lower cost of
52 SWT manufacturers, and the fact that SWTs of different diameters can be readily manufactured using
53 the same forming tools. One of the most widely used product standards internationally for SWTs is
54 API 5L [11]. This is recognized by the International Organization for Standardization (ISO) where
55 continued harmonisation of ISO 3183 [12] with API 5L has led to the 2019 version of this standard
56 only presenting supplementary rules to complement API 5L, thereby resulting in a document that is
57 around six-times shorter than previous versions of ISO 3183.

58 In the construction sector, API 5L products have been successfully used for columns in multi-storey
59 buildings in the Asia-Pacific region for several years. Based on this long experience, the Hong Kong
60 Buildings Department [13] and the Building Construction Authority in Singapore [14] permit the use
61 of API 5L products in the design of steel structures. Whilst full-scale tests on both non-composite and
62 composite columns using SWTs have been conducted, and the results compared with the predictions
63 given by different design standards, the present authors are unaware of any structural reliability
64 analyses that have been undertaken to evaluate the capacity reduction factors required for design.
65 Moreover, given that API 5L SWTs are normally used for conveyance of liquids or gasses, the yield
66 strength of the material is measured in the circumferential direction. As a consequence of this, there
67 is a need to define the required minimum yield strength of the steel in the longitudinal direction when
68 SWTs are designed as columns.

69 The magnitude of the capacity factors given in steel and composite design standards are often based
70 on production control measurements of geometry and yield strength from steel producers that are

71 servicing a particular market at that time [15]. However, if different steel producers subsequently
72 enter the market, this could potentially invalidate the magnitude of the capacity factors previously
73 calculated because the required statistical input values are not normally given in product standards
74 [16]. This issue was recently identified in the RFCS SAFEBRICKTILE project, where it was intended
75 that the statistical properties evaluated for design could be included within future versions of the
76 European product standards [17]. Moreover, there is also a growing need to reuse reclaimed steel in
77 structural applications due to its environmental advantages. In these circumstances, not all of the
78 material and geometrical characteristics are known. Recent design guidance has recommended that
79 more onerous capacity factors than currently given in design standards should be used [18], but these
80 are not based on structural reliability analyses. Conversely, when tensile coupons are taken from the
81 reclaimed steel products and tests are undertaken, a calculation procedure is given to evaluate the
82 characteristic mechanical properties from the results [18], but what impact this has on design
83 resistance of the composite member remains unknown.

84 In the present paper, the sensitivity of the capacity reduction factors for the design models given in
85 NZS 3404.1 [19], AS 4100 [20], AS/NZS 5100.6 [21] and AS/NZS 2327 [4] are investigated when
86 using API 5L [11] products in non-composite and composite column applications. Whilst the focus
87 of this paper is to support SWTs in Australian/New Zealand standards, given that the design models
88 are similar to those used in other international standards, coupled with the fact that the reliability
89 analyses are conducted according to ISO 2394 [22] (in Australia and New Zealand AS 5104 [23] is
90 an identical adoption of ISO 2394), the results from this paper have a wider international relevance.
91 In a similar way as an earlier study that considered the reliability of beams and columns using standard
92 section sizes [24], it is proposed to investigate the sensitivity of using API 5L products by undertaking
93 inverse reliability analyses for each of the design models to identify the minimum number of

94 mechanical tests that would be required to deliver a particular capacity reduction factor. This latter
95 information will be of particular importance to designers when the nominal yield strength of a product
96 is unknown.

97 **1.2 Research objectives**

98 In this study, the following research objectives are identified: (i) experimental databases for steel and
99 steel-concrete composite columns with SWTs are established by collecting data from the literature.
100 Then, reliability analyses are conducted to evaluate the capacity reduction factors for the API 5L [11]
101 steel grades identified below using the design models given in NZS 3404.1 [19], AS 4100 [20],
102 AS/NZS 5100.6 [21] and AS/NZS 2327 [4]. (ii) Inverse reliability analyses are undertaken for each
103 of the design models to identify the minimum number of mechanical tests that will be required to
104 deliver the target capacity reduction factors.

105 Whilst API 5L [11] provides a wide range of sections, from consultation with the industry it was
106 proposed to narrow the scope to include only welded steel (seamed) pipe, considering the cost
107 premium for seamless pipes. On this basis, the study was confined to product specification level 2
108 (PSL 2) pipes which have a maximum f_y/f_u ratio of 0.93, using the following steel grades: X42 (290),
109 X46 (320), X52 (360), X56 (390), X60 (415), X65 (450), X70 (485), and X80 (555) [N.B. The values
110 in the parenthesis indicate the nominal yield strengths in MPa].

111 **2. Reliability based capacity factor calibration**

112 **2.1 Target reliability level**

113 Capacity factors are required to be calibrated to meet the acceptable level of consequences of
114 structural design failure. This acceptable level is described by a target failure probability or a
115 reliability index. The failure probability P_f and the reliability index β has the following relationship:

$$P_f = \Phi(-\beta) \quad (1)$$

116 where Φ is the cumulative distribution function (CDF) of the standardised normal distribution.

117 Both ISO 2394 [22] and AS 5104 [23] suggest that, at the ULS when the failure costs are large and
 118 the relative costs of safety measures are normal, the target reliability index related to a one-year
 119 reference period is $\beta_1 = 4.4$. However, in most design standards around the world the evaluation of
 120 the capacity reduction factors have been based on a 50-year reference period where the previous
 121 version of ISO 2394 [25] and EN 1990 [26] give $\beta_{50} = 3.8$. According to EN 1990, the values of β
 122 for a different reference period can be calculated using the following equation:

$$\Phi(\beta_n) = [\Phi(\beta_1)]^n \quad (2)$$

123 where β_n is the reliability index for a reference period of n years and β_1 is the reliability index for
 124 one-year.

125 From using Eq. (2) it can be seen that for $\beta_{50} = 3.8$ this is equivalent to $\beta_1 = 4.7$. However, considering
 126 that full mutual independence of failure events in subsequent years and expressed as the
 127 multiplications of the terms. This assumption is unrealistic, and it is suggested that $\beta_{50} = 3.8$ can be
 128 more realistically interpreted to be $\beta_1=4.4$ [27]. From this finding, and for consistency with the basis
 129 of international design standards for steel and composite construction, the target reliability index used
 130 in the present paper is based on a 50-year reference period with $\beta_t = \beta_{50} = 3.8$.

131 When we consider a case that the resistance has an unfavourable value without considering the load
 132 effect, this probability has the following relationship with the corresponding reliability index:

$$P(R \leq R_d) = \Phi(-\alpha_d \beta_t) = \Phi(-\beta_R) \quad (3)$$

133 where α_d is the design value for the first-order reliability method (FORM) [28] influence coefficient
134 which has the value of 0.8 according to ISO 2394 [22]/AS 5104 [23], R is the resistance, and R_d is
135 the design resistance.

136 **2.2 Capacity factor calibration procedure considering the effect of statistical uncertainty in** 137 **material tests**

138 The capacity factor calibration procedure proposed in Kang *et al.* [24] based on EN 1990 Annex D.8
139 [26] is used to carry out the following two types of analyses by considering the effect of statistical
140 uncertainty in material tests: (i) forward analysis for calibrating a capacity factor for steel contribution
141 in a structural member; and (ii) inverse analysis to estimate the minimum number of tensile tests for
142 the steel yield strength. This method is selected because it considers that the resistance value always
143 has a non-negative value, and thus it follows a lognormal distribution. This method calibrates capacity
144 factors separately from load factors using the concept of the first-order reliability method (FORM)
145 [27], where sensitivity factors separate the calibration procedures for resistance and load. In this
146 method, the modelling error of the prediction models is statistically estimated from the comparison
147 between the model predictions and the experimental observations for those predictions.

148 In the forward analysis, the capacity factor (ϕ) for a resistance prediction model is defined as follows:

$$\phi = \frac{R_d}{R_n} \quad (3)$$

149 where R_d = the design resistance to meet the target reliability for resistance, and R_n = the nominal
150 resistance.

151 The calculation of these resistance parameters are carried out as follows: let us assume that $g_R(\mathbf{x})$ is a
152 resistance prediction model and \mathbf{x} is a vector of mean-measured values for design parameters. The

153 constant bias of this model can be statistically represented as follows:

$$\bar{b} = \frac{1}{N} \sum_{i=1}^N \left(\frac{R_{ei}}{R_{ii}} \right) \quad (4)$$

154 where N = the number of experimental data, R_{ei} = the resistance observed from the i^{th} specimen in the
155 experiment, and R_{ii} = the resistance predicted by the resistance prediction model $g_R(\mathbf{x}_i)$ for the i^{th}
156 specimen. The unbiased resistance prediction R using this bias correction term is calculated as follows:

$$R = \bar{b} g_R(\mathbf{x}) \delta \quad (5)$$

157 where δ = the modelling error of the unbiased resistance prediction. The modelling error for the i^{th}
158 experiment, δ_i , can be estimated as follows:

$$\delta_i = \frac{R_{ei}}{\bar{b} R_{ii}} \quad (6)$$

159 As it is assumed that R in Eq. (5) follows a lognormal distribution with non-negative values, the
160 coefficient of variation (COV) of R is estimated as follows:

$$V_R \cong \sqrt{\left(V_\delta^2 + V_{Rt,inf}^2 + V_{Rt,finite}^2 \right)} \quad (7)$$

161 where V_δ = the COV of the modelling error estimated using Eq. (6), and $V_{Rt,inf}$ = the COV of the
162 parametric uncertainty for the parameters with an infinite number of experiments, and $V_{Rt,finite}$ = the
163 COV of the parametric uncertainty for the parameters with a finite number of experiments. This
164 equation assumes that the modelling error and the parametric uncertainty are statistically independent.
165 V_{Rt} can be calculated by using the Monte Carlo simulations or the first-order approximations. The
166 standard deviation of $\ln R$ ($\sigma_{\ln R}$) is estimated as follows:

$$\sigma_{\ln R} = \sqrt{\ln(1 + V_R^2)} \quad (8)$$

167 which is used to calculate the design resistance (R_d) in Eq. (3) as follows:

$$R_d = \bar{b}g_R(\mathbf{x}) \exp(-k\sigma_{\ln R} - 0.5\sigma_{\ln R}^2) \quad (9)$$

168 where

$$k = \frac{(k_{d,m}V_\delta^2 + \beta_R V_{Rt,inf}^2 + k_{d,p}V_{Rt,finite}^2)}{V_R^2} \quad (10)$$

169 where $k_{d,m}$ = the fractile factor determined for a finite number of structural member tests, and $k_{d,p}$
 170 = the fractile factor determined for a finite number of structural material tests, to represent the
 171 statistical uncertainty due to the finite number of test data. These factors are for the target reliability
 172 index for resistance (β_R) at the 75% confidence level and can be calculated for unknown $\sigma_{\ln R}$ as
 173 follows:

$$k_d = t_\beta(n-1) \times (1 + 1/n)^{0.5} \quad (11)$$

174 where $t_\beta(n-1)$ is the fractile of the t -distribution for the probability corresponding to β_R . This fractile
 175 factor is used to consider the statistical uncertainty caused by a finite number of tests that is far from
 176 infinity.

177 R_n in Eq. (3) can be calculated using the resistance prediction model $g_R(\mathbf{x}_n)$ by inserting the nominal
 178 input parameters \mathbf{x}_n . When nominal input parameters are not available, the characteristic values based
 179 on the 5% fractile value can alternatively be used [29], or the nominal parameters can be inferred
 180 from the product standard tolerance ranges.

181 The inverse analysis also uses the above-mentioned procedures, and the purpose is not to calibrate

182 the capacity factor for the given target reliability level, but to estimate the minimum required number
183 of material tests to meet the target reliability level for a fixed/given capacity factor [24]. In particular,
184 in the inverse analysis, the number of test samples (n) in Eq. (11) for material tests for the steel tensile
185 strength is estimated. When the capacity factor (ϕ) is fixed or given, Eq. (3) takes the following form:

$$\phi R_n = R_d(n, \mathbf{x}) \quad (12)$$

186 where n is the only unknown term, and it can be numerically solved using optimisation algorithms
187 such as Active-Set Optimisation algorithm [30] and pattern search [31].

188 **3. Forward and inverse reliability analyses for steel and composite columns**

189 The forward and inverse analysis methods presented in the previous section are conducted to estimate
190 the capacity factors and the required minimum number of steel material tests for steel and composite
191 columns, respectively. All the considered columns utilised helical seam pipe, or spirally welded steel
192 tubes (SWTs). The following three types of sections are considered in these analyses: (i) steel hollow
193 sections under pure compression, (ii) concrete-filled steel tubes (CFSTs) under pure compression,
194 and (iii) CFSTs under eccentric loading (combined axial compression and uniaxial bending).

195 One concern of using SWTs in structural applications is whether anisotropy of the steel properties
196 might exist, owing to the fact that the plate rolling direction and the longitudinal axis of the tube are
197 no longer parallel. However, this concern has recently been addressed through two independent
198 investigations on SWTs [32,33], where the results from tensile tests suggest that the material
199 properties may be treated as isotropic. Due to this finding, in the remainder of this paper it is assumed
200 that the yield strength of the steel in SWTs is independent of orientation.

201 **3.1 Parameter uncertainties**

202 All the parameters in the resistance prediction equation have aleatoric uncertainties, and in this study,
 203 they are estimated from the manufacturing tolerances or the literature. The parametric uncertainties
 204 are represented in terms of the bias and scatter, and the manufacturing tolerances for the tube diameter,
 205 thickness, and the tensile strength of steel presented in Tables 1 and 2 are considered to estimate these.
 206 We assume that these parameters are uniformly distributed within the tolerance ranges. It is assumed
 207 that the mean of each parameter is the mid-point of the range, and the standard deviation of each
 208 parameter that is uniformly distributed within the range of the minimum value of r_{min} and the
 209 maximum value of r_{max} is calculated as $(r_{max} - r_{min})/\sqrt{12}$. For all the other parameters that are not
 210 specified in these manufacturing tolerances, the COV values have been taken from the literature such
 211 that the COV of the compressive strength of concrete (f'_c) is taken as 0.10 [34] and the COVs of all
 212 linear dimensions unspecified in the manufacturing tolerances are taken as 0.01 [34].

213 Table 1. Manufacturing tolerances for hollow sections in API specification 5L [11]

Parameter	API 5L	
	Outside dimension for CHS (d_o) (mm)	$d_o \leq 168.3$ $168.3 < d_o \leq 610$ $d_o > 610$
Thickness for CHS (t) (mm)	$t \leq 5.0$ $5.0 < t \leq 15.0$ $t > 15.0$	-0.5 $-0.1 t$ -1.5

214
 215 Table 2. Requirements for the results of tensile tests for PSL 2 pipes in API specification 5L [11]

Pipe grade	Yield strength (MPa)	
	Minimum value	Maximum value
X42 (290)	290	495
X46 (320)	320	525
X52 (360)	360	530
X56 (390)	390	545
X60 (415)	415	565
X65 (450)	450	600
X70 (485)	485	635

X80 (555)	555	705
-----------	-----	-----

216

217 3.2 Steel hollow sections

218 3.2.1 Experimental database

219 Tests on 11 specimens have been collected for SWT columns to estimate the modelling uncertainty
220 statistically, and their input parameters together with their load bearing capacities are provided in
221 Table 3. In the table, D = the diameter of the SWT, t = the thickness of the tube, f_y = the steel yield
222 strength, L_e = the effective length of the column, and P_{max} = the axial load bearing capacity of the
223 column. The experimental data were collected from the following four publications: Akiyama *et al.*
224 [35], Bao *et al.* [36], Gardner [37], and Aslani *et al.* [38]. These data are compared with resistance
225 model predictions, and the modelling error δ_i is statistically estimated using Eq. (6). It should be noted
226 that, in the tests by Aslani *et al.*, the SWTs were manufactured with only single-sided MIG welding
227 on the outside of the pipe, as opposed to the requirement given in API 5L that the welding should be
228 both on the inside and outside. However, given the paucity of experimental data available on SWTs,
229 coupled with the fact that it is likely that any geometrical imperfections introduced from single-sided
230 welding would lead to more conservative resistances, the experimental data presented in Table 3 were
231 first assumed to belong to the same population within the reliability analyses. To investigate whether
232 this assumption was reasonable, the data was subsequently split into subsets corresponding to the
233 welding method and the reliability analyses repeated.

234 Table 3. Experimental database for spirally welded steel tube columns under axial compression

Article	Specimen	D (mm)	t (mm)	f_y (MPa)	L_e (mm)	P_{max} (kN)
Akiyama <i>et al.</i> [35]	SA-7	400	7	409	1600	3360
	SA-9	400	9	470	1600	5350
Bao <i>et al.</i> [36]	c-st-1	323	6	344.35	970	1980
	c-st-2	323	6	344.35	970	1990
Gardner [37]	9	168.8	2.64	298.12	1730	412.66

	10	169.3	2.64	317.74	1730	365.79
Aslani <i>et al.</i> [38]	H0SWT102-S	103.05	1.9	288	300	183.6
	H0SWT152-S	152.75	1.9	288	450	221.93
	H0SWT203-S	204.25	1.9	288	600	274.5
	H0SWT254-S	251.75	1.9	288	750	320.4
	H0SWT203-L	203	1.9	288	1400	296.8

235

236 3.2.2 Resistance prediction models

237 In NZS 3404.1 [19], AS 4100 [20], and AS/NZS 5100.6 [21], the nominal section capacity (N_s) of a
 238 steel column under axial compression is predicted as follows:

$$N_s = \phi k_f A_n f_y \quad (13)$$

239 where ϕ = the capacity factor for steel with a value of 0.9; k_f = the form factor defined as a ratio of
 240 the effective to the gross areas of the section; A_n = the nominal area of the steel sections; and f_y = the
 241 nominal yield strength of the structural steel.

242 The ultimate member capacity (N_c) of a steel column under pure axial compression is predicted as
 243 follows:

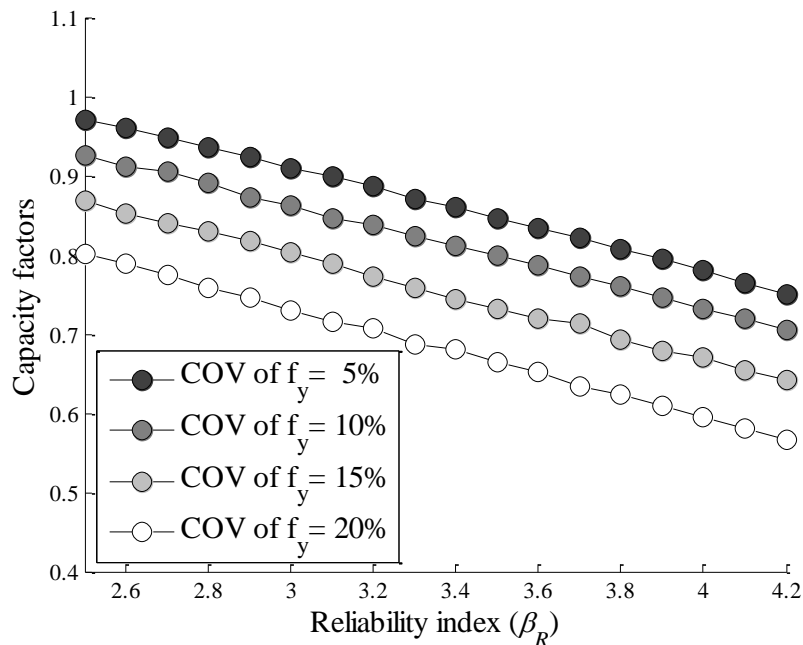
$$N_c = \alpha_c N_s \leq N_s \quad (14)$$

244 where α_c = the member slenderness reduction factor calculated according to NZS 3404.1, AS 4100,
 245 and AS/NZS 5100.6.

246 3.2.3 Analysis results

247 The calibrated capacity factors for steel in the circular hollow sections under axial loading are plotted
 248 in Figure 1. The forward analysis procedure introduced in the previous section is used. The capacity
 249 factors are calculated for the target reliability index β_R for resistance values, for the range of 2.5-4.2.

250 The analyses are repeated for different COV values of steel yield strength. As expected, the capacity
 251 factor values decrease as the target reliability level increases and the COV of steel yield strength
 252 increases. For the COV of steel yield strength of 7% [39] and $\beta_R = 3.04$ (see Eq. (3)), the estimated
 253 capacity factor has a value of 0.893 (see Table 4), which is close to the value of 0.90 provided in
 254 NZS 3404.1, AS 4100, and AS/NZS 5100.6. This means that the capacity factor provided in the
 255 current design standards just meets the desired target reliability level, but it does not have extra safety
 256 or redundancy over the target reliability level. This is different from the design of other member types
 257 or failure modes that usually have additional safety or conservatism by using capacity factors. This
 258 is observed especially in the design of hollow section columns under axial compression, because the
 259 effect of the uncertainty in the section thickness directly and significantly affects the overall
 260 parametric uncertainty of a member. This observation is consistent with the findings presented by
 261 Kang *et al.* [24] for rectangular hollow sections under axial compression.



262

263 Figure 1. Calibrated capacity factor for steel in spirally welded steel tube columns under axial
 264 compression for various COV of the steel yield strength
 265

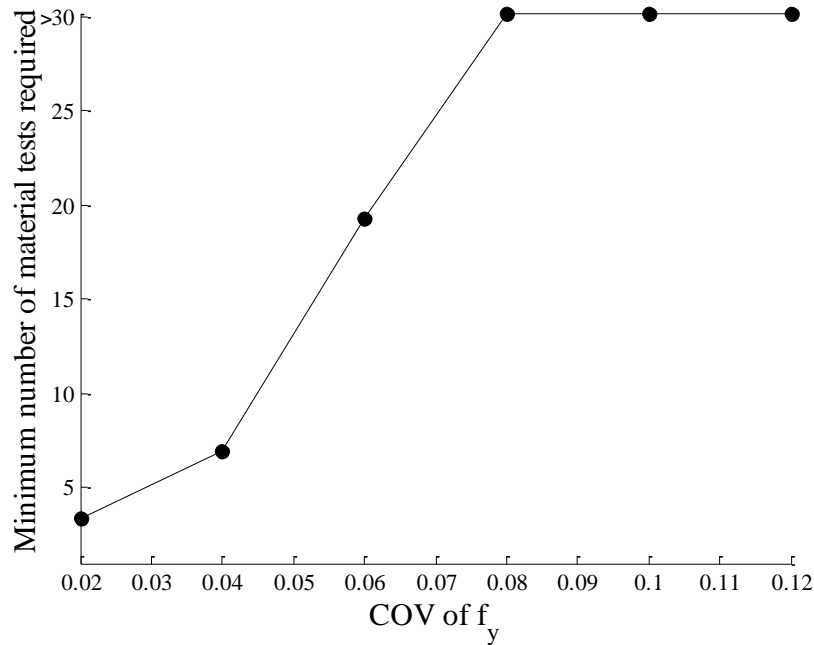
266 To investigate whether it was reasonable to include the experimental data with single-sided welding,
 267 the data was split into subsets corresponding to the welding method, and the reliability analyses were
 268 repeated with a COV for steel yield strength of 7% and $\beta_R = 3.04$ (see Table 4). To ensure a fair
 269 comparison, the capacity factor ϕ values are calculated by assuming that the fractile $k_{d,m}$ evaluated for
 270 the combined data (see Eq. (3)), remains constant in order not to introduce any additional statistical
 271 uncertainty. As can be seen from Table 4, the values of bias and overall error are relatively insensitive
 272 to the welding method. From this simple comparison, it appears that the initial assumption made in
 273 Section 3.2.1 that the inclusion of the single-sided welding data would lead to more conservative
 274 design resistances is reasonable, which is reflected in the lower capacity factor value in Table 4.

275 Table 4. Comparison of uncertainties and capacity factor for steel hollow sections under axial
 276 compression

	n (number of tests)	\bar{b} (bias)	V_δ (Model error)	V_{Rt} (Parametric error)	V_R (overall error)	ϕ
All	11	0.993	0.064	0.083	0.105	0.893
Double-sided welding	6	0.984	0.068	0.083	0.108	0.906
Single-sided welding	5	1.004	0.064	0.084	0.105	0.861

277
 278 Next, the inverse analysis according to the procedure provided in the previous section has been carried
 279 out, and the minimum number of steel tensile tests required to meet the target value of $\beta_R = 3.04$ have
 280 been calculated. The analyses have been repeated for the COV of f_y values with the range of 2-12%.
 281 The results are plotted in Figure 2, and it shows an increasing trend of the required number of material
 282 tests according to the increasing COV of f_y , as the uncertainty of the resistance prediction increases,
 283 the statistical uncertainty due to the insufficient amount of material tests should be reduced to keep
 284 the target reliability level. The proposed number of required steel material tests are also tabulated in
 285 Table 5 according to this analysis for practical purposes. As can be seen, more than 30 tests are

286 required when the observed COV of the material tests is greater than 8%. This finding is because the
 287 resistance model has a very small conservatism and just meets the target reliability level even with
 288 infinite material tests.



289
 290 Figure 2. The minimum number of required steel material tests to meet the target reliability level for
 291 spirally welded steel hollow tubes under axial compression
 292

293 Table 5. Recommended number of steel yield strength tests for spirally welded hollows sections
 294 under axial compression (based on $f_{ym}/f_{yn} = 1.35$)

COV of f_y	2%	4%	6%	$\geq 8\%$
# of tests	3	7	19	>30

295
 296 **3.3 CFST sections under axial compression**

297 *3.3.1 Experimental database*

298 A total of 41 specimens have been collected for CFSTs with SWTs under axial compression. The
 299 input parameters and load bearing capacities are provided in Table 6, where f_{cm} is the mean measured
 300 concrete compressive strength. The experimental data were collected from the following six
 301 publications: Wang *et al.* [40], Aslani *et al.* [38], Akiyama *et al.* [35], Gardner [37], Gunawardena *et*

302 *al.* [41], and Gunawardena and Aslani [42]. However, in the tests by Aslani *et al.* together with
303 Gunawardena and Aslani, the SWTs were manufactured with only a single-sided MIG welding on
304 the outside of the pipe (as opposed to the requirement given in API 5L that the welding should be
305 both on the inside and outside of the pipe). For the same reasons given in Section 3.2.1, the
306 experimental data presented in Table 6 were initially assumed to belong to the same population within
307 the reliability analyses. However, to investigate whether this assumption was reasonable, the data was
308 again split into subsets corresponding to the welding method and the reliability analyses subsequently
309 repeated.

310 For the cases when the mean measured cylinder compressive strength of concrete (f_{cm}) values are not
311 provided in the experimental data, but only the cube strength (f_{cu}) are provided instead, the conversion
312 table provided by Yu *et al.* [43] was used, which represents the approximate relationship between the
313 cylinder strength (f_{cm}) and the cube strength (f_{cu}).

314 Table 6. Experimental database for CFSTs under axial compression

Article	Specimen	D (mm)	t (mm)	f_y (MPa)	f_{cm} (MPa)	L_e (mm)	P_{max} (kN)
Wang <i>et al.</i> [40]	CD4-1	425.8	5.2	259.8	42.51	1278	10523
	CD4-2	427.1	5.1	259.8	42.51	1278	10784
	CD6-1	628.5	6.9	276	42.51	1890	21207
	CD6-2	628	7.1	276	42.51	1890	21582
	CD8-1	817.4	9	278.8	42.51	2460	36933
	CD8-2	820.8	9.3	278.8	42.51	2460	37221
Aslani <i>et al.</i> [38]	C-SWT102-S	103	1.9	288	38.78	300	609.81
	C-SWT152-S	152.25	1.9	288	38.78	450	1044.92
	C-SWT203-S	204	1.9	288	38.78	600	1788
	C-SWT254-S	252	1.9	288	38.78	750	2525
	C-SWT203-L	203.25	1.9	288	38.78	1400	1698
Akiyama <i>et al.</i> [35]	SB20-7	400	7	409	21.7	1600	6740
	SB20-9	400	9	470	25.6	1600	9510
	SB60-9	400	9	470	40.5	1600	12494
Gardner [37]	1a	168.8	2.64	298.12	17.95	305	1323.9
	2a	168.8	2.64	298.12	34.13	305	1220.93
	3a	169.3	2.62	317.74	36.58	305	1304.28

	4a	169.3	2.62	317.74	33.54	305	1328.8
	5a	168.3	3.6	221.63	26.58	305	1559.26
	6a	168.3	3.6	221.63	32.75	305	1431.77
	6b	168.3	3.6	221.63	32.95	305	1461.19
	7a	168.8	5	260.86	32.95	305	1961.33
	7b	168.8	5	260.86	32.95	305	1966.23
	8a	168.8	5	260.86	27.46	305	2010.36
	8b	168.8	5	260.86	27.46	305	2010.36
	1	168.8	2.64	298.12	17.95	1830	823.76
	2	168.8	2.64	298.12	34.13	1830	916.92
	3	169.3	2.62	317.74	36.58	1830	757.07
	4	169.3	2.62	317.74	33.54	1830	690.39
	5	168.3	3.6	221.63	26.58	1830	947.32
	6	168.3	3.6	221.63	32.75	1830	1049.31
	7	168.8	5	260.86	32.95	1830	1132.67
	8	168.8	5	260.86	27.46	1830	1166.99
Gunawardena <i>et al.</i> [41]	LD1E0	102.67	1.83	234.9	24.20	1226	304
	LD2E0	152.74	1.76	234.9	23.05	1676	570
	LD3E0	203.04	1.93	234.9	24.34	2135	996
	LD4E0	229.81	1.96	234.9	24.22	2594	1228
Gunawardena and Aslani [42]	D1E0	102.9	1.83	234.9	29.9	614	363
	D2E0	152.7	1.95	234.9	30.4	764	740
	D3E0	202.9	1.92	234.9	31.1	917	1249
	D4E0	230.0	1.94	234.9	29.3	1070	1495

315

316 3.3.2 Resistance prediction models

317 In AS/NZS 5100.6 [21] and AS/NZS 2327 [4], the design ultimate section capacity (N_{us}) for a circular
318 CFST column under axial compression is given as:

$$N_{us} = \phi A_s \eta_2 f_y + \phi A_c f'_c \left(1 + \frac{\eta_1 f_y}{d_0 f'_c} \right) \quad (15)$$

319 where A_s and A_c = the areas of the steel and concrete sections, respectively; f_y = the nominal yield
320 strength of the steel; f'_c = the characteristic compressive strength of the concrete; ϕ and ϕ_c = the
321 capacity reduction factors for steel and concrete, respectively (with the existing target values given
322 as 0.9 and 0.65); and η_1 and η_2 = the coefficients accounting for the confinement effect (where η_1
323 represents the concrete strength increase, and η_2 represents the steel strength reduction).

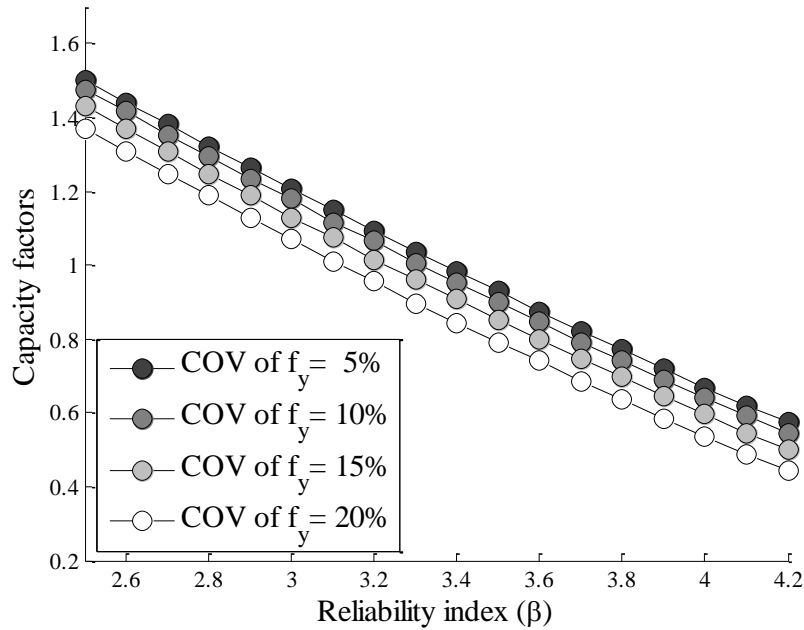
324 The design ultimate member capacity (N_{uc}) of CFST is given as follows:

$$N_{uc} = \alpha_c N_{us} \leq N_{us} \quad (16)$$

325 For a stub column defined by L_e/d_o or $L_e/b \leq 4$, in which L_e = the effective length of a column and
326 b = the section width of a rectangular tube, $\alpha_c = 1$.

327 3.3.3 Analysis results

328 The forward analysis results for CFSTs with SWTs under axial compression are presented in Figure
329 3. The analyses are repeated for the target reliability index β for resistance values, for the range of
330 2.5-4.2 and for different COV values of steel yield strength. The results are more sensitive to the
331 target reliability level as shown by the steeper slopes because there are two materials in CFSTs, and
332 two types of capacity factors are included in the resistance model (i.e. one for steel and one for
333 concrete). When the concrete capacity factor is fixed, it is more difficult to change the reliability level
334 by changing the steel capacity factor alone compared to the case when there is only one capacity
335 factor in the whole design equation. Due to this issue, the increase of the COV of f_y does not
336 significantly reduce the capacity factor values because this uncertainty in f_y affects the steel
337 contribution only. The capacity factor value for steel with a COV of $f_y = 7\%$ [39] is estimated as 1.194
338 when the capacity factor for concrete is fixed at 0.65 (see Table 7), which is greater than 0.90 provided
339 in AS/NZS 5100.6 [21] and AS/NZS 2327 [4]. This shows that the design model has extra safety
340 above the target reliability level, thereby providing a safe design.



341

342 Figure 3. Calibrated capacity factor for steel in CFSTs with spirally welded steel tubes for various
 343 COV of the steel yield strength

344

345 To investigate whether it was reasonable to include the experimental data with single-sided welding,
 346 the data was split into subsets corresponding to the welding method, and the reliability analyses were
 347 repeated with a COV for steel yield strength of 7% and $\beta_R = 3.04$ (see Table 7). Again, to ensure a
 348 fair comparison, the capacity factor ϕ values are calculated by assuming that the fractile $k_{d,m}$ evaluated
 349 for the combined data (see Eq. (3)), remains constant in order not to introduce any additional statistical
 350 uncertainty. As can be seen from Table 7, the biases are overall similar for all data, double-sided
 351 welding, and single-sided welding. However, the modelling error of the single-sided welded
 352 specimens is lower than the other specimens, which is considered to be caused by the random nature
 353 of the data from the smaller sample size, together with better controlled experiments that were
 354 undertaken within the same laboratory. Notwithstanding this, the overestimation of the capacity factor
 355 does not much affect the overall capacity factor and, the calculated capacity factor is already well
 356 above the target value of 0.90 given in AS/NZS 5100.6 and AS/NZS 2327. It is concluded that the
 357 addition of the single-sided welding data reduces the overall statistical error and the associated extra

358 safety margin.

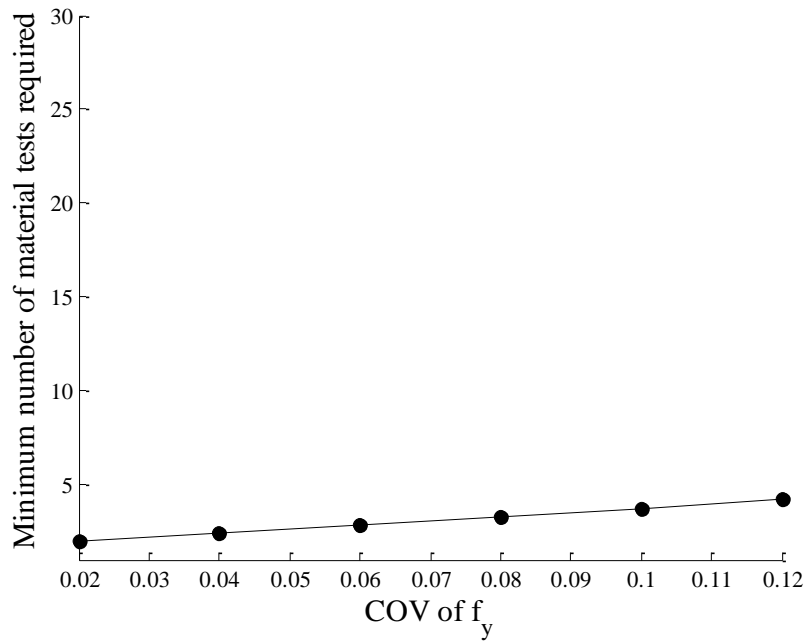
359 Table 7. Comparison of uncertainties and capacity factor for CFST sections under axial
360 compression

	n (number of tests)	\bar{b} (bias)	V_{δ} (Model error)	V_{Rt} (Parametric error)	V_R (overall error)	ϕ (without extra statistical error)
All	41	1.041	0.142	0.067	0.158	1.194
Double-sided welding	28	1.058	0.164	0.064	0.176	1.046
Single-sided welding	13	1.003	0.121	0.072	0.141	1.310

361

362 Next, the inverse analyses have been carried out for CFST columns with SWTs. The results are shown
363 in Figure 4. As the design model for CFST columns has extra safety due to the conservatism that
364 exists within the equation and the capacity factors, the required material test numbers are quite low
365 to achieve the target reliability level for resistance with $\beta_R = 3.04$. The shallow slope of the graph
366 shows that the statistical uncertainty due to the number of material tests does not significantly affect
367 the overall reliability of the design, compared to other types of uncertainties such as parametric and
368 modelling uncertainties. The proposed required material test numbers are also tabulated in Table 8
369 for practical purposes.

370



371

372 Figure 4. The minimum number of required steel material tests to meet the target reliability level for
 373 CFSTs under axial compression

374

375 Table 8. Recommended number of steel yield strength tests for CFST with spirally welded tubes
 376 under axial compression (based on $f_{ym}/f_{yn} = 1.35$)

COV of f_y	2%	4%	6%	8%	10%	12%
# of tests	2	2	3	3	4	4

377

378 3.4 CFST sections under axial compression and uniaxial bending

379 3.4.1 Experimental database

380 A total of 16 specimens have been collected for CFSTs with SWTs under axial compression and
 381 uniaxial bending due to eccentric loading (see Table 9). The experimental data were collected from
 382 the following two publications: Gunawardena *et al.* [41] and Gunawardena and Aslani [42]. The
 383 uniaxial bending occurs due to the loads applied with the eccentricity of either at $0.15D$ or $0.40D$.
 384 The SWTs for these tests were manufactured with only a single-sided MIG welding on the outside of
 385 the pipe (as opposed to the requirement given in API 5L that the welding should be both on the inside
 386 and outside of the pipe). However, from the comparisons of the uncertainties and capacity factors for
 387 the different welding methods presented in Section 3.2.3 and 3.3.2, coupled with the lack of

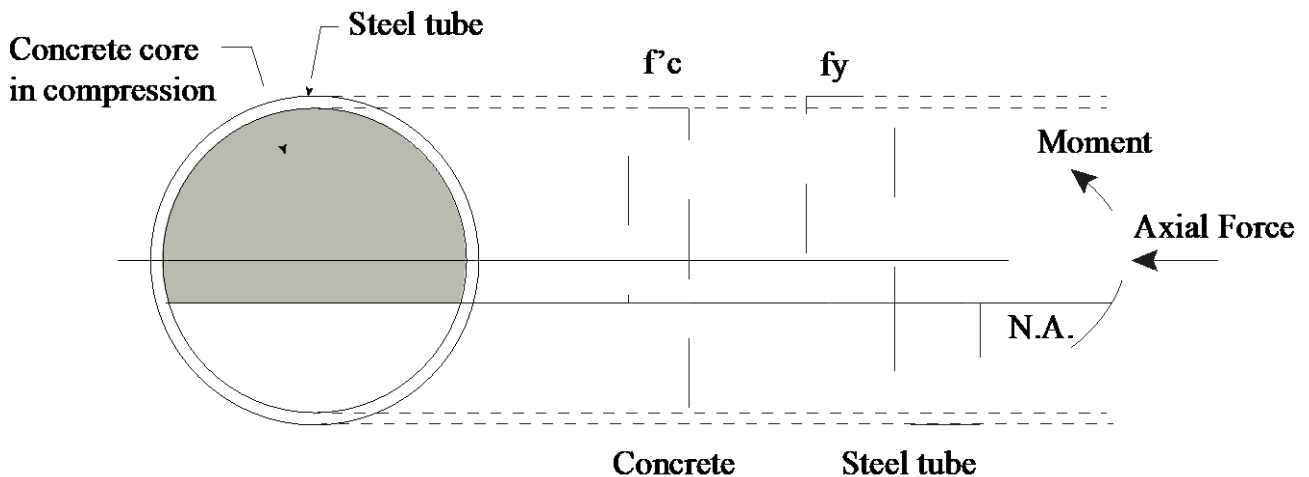
388 experimental data available, it is assumed that the results are insensitive to the welding method.

389 Table 9. Experimental database for CFSTs under axial compression and uniaxial bending

Article	Specimen	D (mm)	t (mm)	f_y (MPa)	f_{cm} (MPa)	L_e (mm)	M_{max} (kNm)	P_{max} (kN)	e (mm)
Gunawardena <i>et al.</i> [41]	LD1E1	102.77	1.77	234.9	24.2	1226	5.8	254	$0.15D$
	LD1E2	102.72	1.83	234.9	24.18	1226	8.1	162	$0.40D$
	LD2E1	152.76	1.78	234.9	23.15	1676	13.7	421	$0.15D$
	LD2E2	152.72	1.81	234.9	23.15	1676	20	269	$0.40D$
	LD3E1	202.99	1.95	234.9	24.27	2135	25.4	601	$0.15D$
	LD3E2	202.15	1.93	234.9	24.34	2135	33.6	351	$0.40D$
	LD4E1	229.69	1.98	234.9	24.25	2594	33.9	723	$0.15D$
	LD4E2	230.14	1.95	234.9	24.25	2594	43.7	395	$0.40D$
Gunawardena and Aslani [42]	D1E1	102.9	1.88	234.9	29	614	4.8	298	$0.15D$
	D1E2	102.9	1.86	234.9	29.9	614	8.9	195	$0.40D$
	D2E1	152.7	2.1	234.9	30.4	764	15.1	557	$0.15D$
	D2E2	153	1.99	234.9	30.4	764	21.7	327	$0.40D$
	D3E1	202.8	1.86	234.9	31.1	917	27.1	778	$0.15D$
	D3E2	202.7	1.85	234.9	31.1	917	38.2	445	$0.40D$
	D4E1	229.5	1.86	234.9	29.7	1070	37.9	939	$0.15D$
	D4E2	229.7	1.93	234.9	29.3	1070	51.1	522	$0.40D$

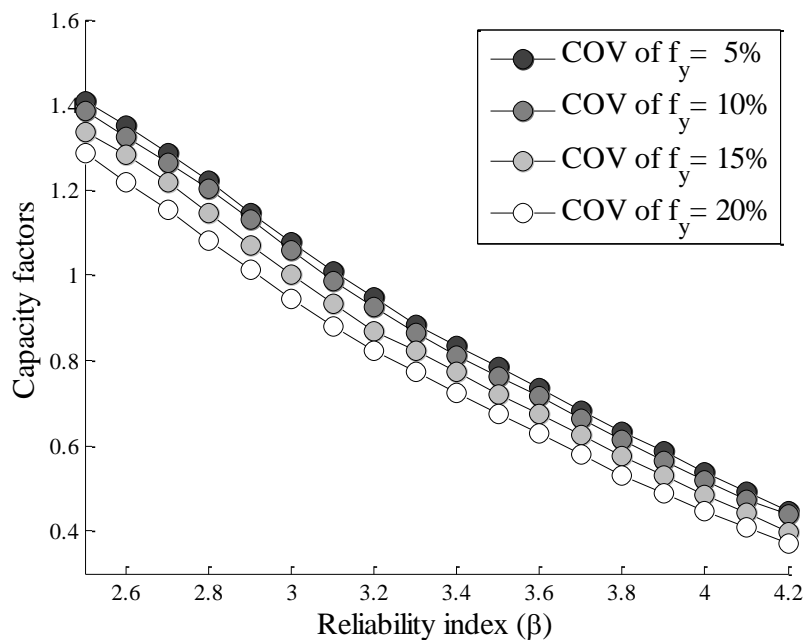
390 3.4.2 Resistance prediction models

391 The axial and moment resistance of a CFST column under axial compression and uniaxial bending is
 392 derived from the moment axial load (M-N) interaction curves where $M = N \cdot e_{eff}$, considering the
 393 effective increase of eccentricity because of the 2nd order effects, and e_{eff} = effective eccentricity. The
 394 interaction curve is derived from the stress distributions along the section as shown in Figure 5.



395
 396 Figure 5 Stress blocks for calculation of a moment axial load capacity interaction curve

398 The forward analysis results for CFSTs with SWTs under axial compression and uniaxial bending are
 399 presented in Figure 6. The forward analysis results show the reliability level similar to the CFSTs
 400 under axial compression. The slope is steep, similar to the case of CFSTs under axial compression,
 401 which is due to the fixed concrete capacity factor that gives a constant amount of safety. A greater
 402 change in a steel capacity factor is needed to change the overall reliability level. The capacity factor
 403 value for steel for the COV of $f_y = 7\%$ [39] is estimated as 1.081 when that for concrete is fixed at
 404 0.65, which is greater than 0.90 provided in NZS 3404.1 [19], AS 4100 [20], AS/NZS 5100.6 [21]
 405 and AS/NZS 2327 [4]. This means that the design model provides extra safety against the target
 406 reliability level.



407

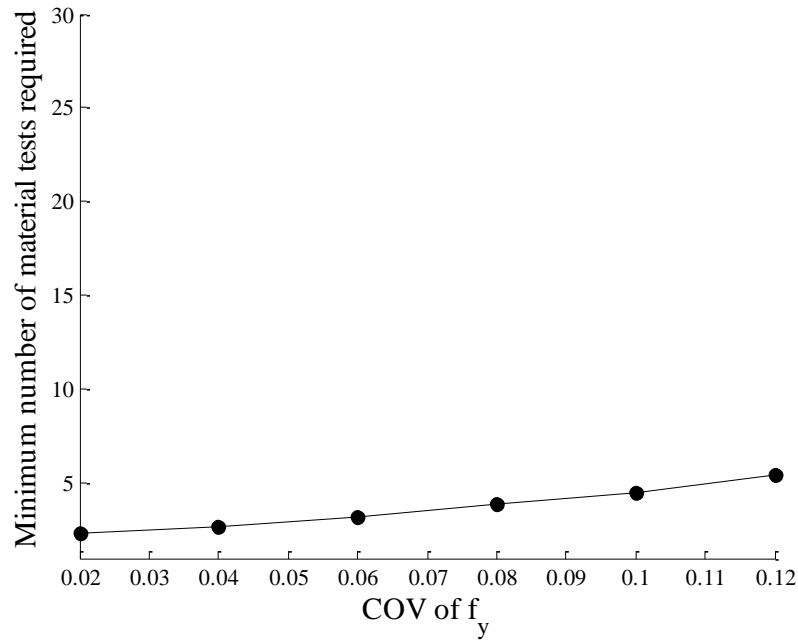
408 Figure 6. Calibrated capacity factor for steel in CFSTs with spirally welded steel tubes under axial
 409 compression and uniaxial bending for various COV of the steel yield strength

410

411 The inverse analysis results are shown in Figure 7. The range of COVs of steel yield strength from
 412 4% and 12 % have been considered. The trend is similar to CFST under axial compression, and it

413 requires a slightly greater number of material tests compared to that for CFST under axial
 414 compression. It is also shown that the effect of COV of f_y is similar to that of CFST under axial
 415 compression. The proposed numbers of required material tests are also tabulated in Table 10 for
 416 practical purposes.

417



418

419 Figure 7. The minimum number of required steel material tests to meet the target reliability level for
 420 CFSTs under axial compression and uniaxial bending

421

422 Table 10. Recommended number of steel yield strength tests for CFST with spirally welded tubes
 423 under eccentric loading (based on $f_{ym}/f_{yn} = 1.35$)

COV of f_y	2%	4%	6%	8%	10%	12%
# of tests	2	3	3	4	4	5

424

425 4. Conclusion

426 This study carried out the capacity factor calibration for the design of steel and steel-concrete
 427 composite columns with helical seam pipe, which are also known as spirally welded steel tubes
 428 (SWTs). The analysis included the forward analysis to calibrate the capacity factor for steel, and the
 429 inverse reliability analysis to estimate the required number of material tests to meet the target

430 reliability level for given capacity factors. This latter information will be of particular importance to
431 designers when the nominal yield strength of a product is unknown, as may occur when reclaimed
432 steel is reused. The following three types of members with circular cross-sections were considered:
433 (i) columns under axial compression, (ii) CFST columns under axial compression, and (iii) CFST
434 columns under combined axial compression and uniaxial bending due to eccentric loading.

435 For the SWT columns, 11 data were collected and used to estimate the modelling error. The design
436 equation gave the reliability just close to the target reliability index for resistance. This was because
437 of the effect of the uncertainty in thickness that directly affected the reliability and also the statistical
438 error due to the number of tests far from infinity. The inverse analysis results showed that the required
439 number of steel tensile tests quickly increased as the measured COV of f_y from the limited number of
440 material tests increased. For the CFST columns with SWTs under axial compression, 41 data were
441 collected and used to estimate the modelling error. The reliability achieved by the resistance model
442 was greater than the target reliability level showing the conservatism of the model. The inverse
443 analysis results showed that the required number of material tests did not quickly increase according
444 to the measured COV of f_y from the limited number of material tests, as the high reliability level was
445 already achieved by the design model itself. For the CFST columns with SWTs under axial
446 compression and uniaxial bending, 16 data were collected and used to estimate the modelling error.
447 The reliability achieved by the resistance model was similar to that of CFSTs under pure axial
448 compression and still higher than the target reliability level, showing the conservatism of the model.
449 The inverse analysis trend was similar to that of CFSTs under pure axial compression and it required
450 a slightly increased number of material tests to meet the target reliability level.

451 Some of the test specimens considered in this study consisted of SWTs manufactured with only
452 single-sided MIG welding on the outside of the pipe (as opposed to the requirement given in API 5L

453 that the welding should be both on the inside and outside of the pipe). From splitting the data into
454 subsets corresponding to the welding method, reliability analyses were repeated for SWTs and CFSTs
455 under axial compression. Whilst the test data is limited, the results suggest that the inclusion of test
456 specimens with single-sided welding leads to more conservative design resistances. However, the
457 calculated capacity factors generally still achieve similar or higher target values than provided by the
458 current Australian and New Zealand design standards. Notwithstanding this, the authors were unable
459 to find any test data for double-sided welded CFSTs subjected to combined axial compression and
460 uniaxial bending. As a consequence of this, further tests on members with different fabrication
461 methods are encouraged.

462

463 **Acknowledgements**

464 Financial support for this investigation was provided by the New Zealand Heavy Engineering
465 Research Association (HERA), which is gratefully acknowledged. Also, thanks go to Steel
466 Construction New Zealand (SCNZ) for supporting the background work conducted by the second
467 author whilst in his former role at HERA.

468 **References**

- 469 [1] M. Shams, M.A. Saadeghvaziri, State of the art of concrete-filled steel tubular columns,
470 *Structural Journal*. 94 (1997) 558–571.
- 471 [2] H.G. Prion, J. Boehme, Beam-column behaviour of steel tubes filled with high strength
472 concrete, *Canadian Journal of Civil Engineering*. 21 (1994) 207–218.
- 473 [3] L.-H. Han, W. Li, R. Bjorhovde, Developments and advanced applications of concrete-filled
474 steel tubular (CFST) structures: Members, *Journal of Constructional Steel Research*. 100
475 (2014) 211–228.

- 476 [4] Standards Australia International Ltd./Standards New Zealand, AS/NZS 2327: 2017
477 Composite structures - Composite steel-concrete construction in buildings, New South
478 Wales/Wellington, Australia/New Zealand, 2017.
- 479 [5] European Committee for Standardization (CEN), EN 1994-1-1 Eurocode 4: Design of
480 composite steel and concrete structures – Part 1-1: General rules and rules for buildings,
481 Brussels, 2004.
- 482 [6] American Institute of Steel Construction (AISC), AISC 360-16, Specification for Structural
483 Steel Buildings, Chicago, 2016.
- 484 [7] S.K. Azad, B. Uy, Effect of concrete infill on local buckling capacity of circular tubes, Journal
485 of Constructional Steel Research. 165 (2020) 105899.
- 486 [8] C.W. Roeder, D.E. Lehman, E. Bishop, Strength and stiffness of circular concrete-filled tubes,
487 Journal of Structural Engineering. 136 (2010) 1545–1553.
- 488 [9] Hicks SJ, Newman GM, Edwards M, Orton A. Design guide for SHS concrete filled columns,
489 CT 26, Corus Tubes Structural & Conveyance Business, Corby, UK, 2005, p. 62.
- 490 [10] Y. Gunawardena, F. Aslani, Behaviour and design of concrete-filled mild-steel spiral welded
491 tube short columns under eccentric axial compression loading, Journal of Constructional Steel
492 Research. 151 (2018) 146–173.
- 493 [11] American Petroleum Institute (API). API Specification 5L, Specification for Line Pipe, 46th
494 Edition, April 2018.
- 495 [12] International Organization for Standardization (ISO), ISO 3183: 2019 Petroleum and natural
496 gas industries — Steel pipe for pipeline transportation systems. Geneva, 2019.
- 497 [13] Code of Practice for the Structural use of Steel, The Government of Hong Kong Special
498 Administrative Region, Buildings Department, Hong Kong, 2011
499 [https://www.bd.gov.hk/doc/en/resources/codes-and-references/code-and-design-](https://www.bd.gov.hk/doc/en/resources/codes-and-references/code-and-design-manuals/SUOS2011.pdf)
500 [manuals/SUOS2011.pdf](https://www.bd.gov.hk/doc/en/resources/codes-and-references/code-and-design-manuals/SUOS2011.pdf) (accessed 9 April 2021)
- 501 [14] BC1: 2012. Design guide on use of alternative structural steel to BS 5950 and Eurocode 3.
502 Building and Construction Authority (BCA), Singapore, 2012
503 [https://www1.bca.gov.sg/docs/default-source/docs-corp-regulatory/building-](https://www1.bca.gov.sg/docs/default-source/docs-corp-regulatory/building-control/design_guide_bc1_2012.pdf)
504 [control/design_guide_bc1_2012.pdf](https://www1.bca.gov.sg/docs/default-source/docs-corp-regulatory/building-control/design_guide_bc1_2012.pdf) (accessed 9 April 2021)

- 505 [15] Charbrolin B, Partial Safety Factors for Resistance of Steel Elements to EC3 and EC4 –
506 Calibration for Various Steel Products and Failure Criteria. Office for Official Publications of
507 the European Communities, Luxembourg, 2002.
- 508 [16] Hicks S. Eurocodes – Overcoming the barriers to global adoption. Proceedings of the
509 Institution of Civil Engineers, Civil Engineering. 2015, 168(4), pp. 179-184
- 510 [17] Simões da Silva L, Marques L, Tankova T, Rebelo C, Kuhlmann U, Kleiner A, Spiegler J,
511 Snijder HH, Dekker RWA, Dehan V, Taras A, Haremza C, Cajot L-G, Vassart O, Popa N.
512 Standardization of Safety Assessment Procedures across Brittle to Ductile Failure Modes
513 (SAFEBRITILE), Publications Office of the European Union, Luxembourg, 2017.
- 514 [18] Brown DG, Pimentel RJ, Sansom MR. Structural steel reuse - Assessment, testing and design
515 principles, SCI P 427, Steel Construction Institute, Ascot, UK, 2019.
- 516 [19] Standards New Zealand, NZS 3404.1: 2009. Part 1: Steel structures standard, Wellington,
517 New Zealand, 2009.
- 518 [20] Standards Australia International Ltd., AS 4100:1998 (R2016) Steel Structures, New South
519 Wales, Australia, 2016.
- 520 [21] Standards Australia International Ltd./Standards New Zealand, AS/NZS 5100.6: 2017
521 Bridge design – Part 6: Steel and composite construction, New South Wales/Wellington,
522 Australia/New Zealand, 2017.
- 523 [22] International Organization for Standardization (ISO), ISO 2394: 2015 General principals on
524 reliability for structures. Geneva, 2015.
- 525 [23] Standards Australia International Ltd., AS 5104: 2017 General principles on reliability for
526 structures, New South Wales, Australia, 2017.
- 527 [24] W.-H. Kang, S.J. Hicks, B. Uy, A. Fussell, Design resistance evaluation for steel and steel-
528 concrete composite members, Journal of Constructional Steel Research. 147 (2018) 523–548.
- 529 [25] International Organization for Standardization (ISO), ISO 2394: 1998 General principals on
530 reliability for structures. Geneva, 1998.
- 531 [26] European Committee for Standardization (CEN), EN 1990: 2002 Eurocode: Basis of
532 structural design, Brussels, 2002.
- 533 [27] Vrouwenvelder ACWM. Developments towards full probabilistic design codes, Structural
534 Safety. 24 (2002) 417-432

- 535 [28] A. Der Kiureghian, First-and second-order reliability methods, Engineering Design
536 Reliability Handbook. 14, 2005.
- 537 [29] W.-H. Kang, S. Hicks, B Uy, Safety factors for the resistance of steel sections. Australian
538 Journal of Structural Engineering, 16 (2) (2015) 116.
- 539 [30] J. Nocedal, S. Wright, Numerical optimization. Springer Science & Business Media, New
540 York, USA, 2006.
- 541 [31] C. Audet, J.E. Dennis, Analysis of generalized pattern searches. SIAM Journal on
542 Optimization. 13 (3) (2002) 889-903.
- 543 [32] A. Sadowski, J. Rotter, T. Reinke, T. Ummenhofer, Analysis of variance of tensile tests from
544 spiral welded carbon steel tubes, Construction and Building Materials. 75 (2015) 208–212.
- 545 [33] D. Li, B. Uy, F. Aslani, Behaviour and design of spiral-welded stainless steel tubes subjected
546 to axial compression, Journal of Constructional Steel Research. 154 (2019) 67-83
- 547 [34] W.-H. Kang, B. Uy, Z. Tao, S. Hicks, Design strength of concrete-filled steel columns,
548 Advanced Steel Construction. 11 (2015) 165–184.
- 549 [35] M. Akiyama, H. Naito, K. Ono, N. Shirahama, D. Matsumoto, M. Suzuki, Concentric
550 loading tests of concrete filled spiral steel tubes and stress-strain relation of concrete confined
551 by steel tubes, Doboku Gakkai Ronbunshuu E (土木学会論文集 E). 65 (2009) 548–563.
- 552 [36] Y. Bao, Z. Jing, C. Yiyi, S. Zuyan, Experiment on spiral welded stub columns of pipes and
553 tubes, Steel Construction. 1 (2002).
- 554 [37] N.J. Gardner, Use of spiral welded steel tubes in pipe columns, in: Journal Proceedings,
555 1968: pp. 937–942.
- 556 [38] F. Aslani, B. Uy, J. Hur, P. Carino, Behaviour and design of hollow and concrete-filled spiral
557 welded steel tube columns subjected to axial compression, Journal of Constructional Steel
558 Research. 128 (2017) 261–288.
- 559 [39] Joint Committee on Structural Safety (JCSS), JCSS Probabilistic Model Code.
560 <https://www.jcss-lc.org/jcss-probabilistic-model-code/> (accessed on 22 May 2020), 2001.
- 561 [40] W. Wang, Z. Tang, Z. Li, H. Ma, Bearing capacities of different-diameter concrete-filled
562 steel tubes under axial compression, Advances in Materials Science and Engineering. 2016.
- 563 [41] Y. Gunawardena, F. Aslani, B. Uy, Behaviour and design of concrete-filled mild-steel spiral
564 welded tube long columns under eccentric axial compression loading, Journal of
565 Constructional Steel Research. 159 (2019) 341–363.

- 566 [42] Y. Gunawardena, F. Aslani, Behaviour and design of concrete-filled mild-steel spiral welded
567 tube short columns under eccentric axial compression loading, *Journal of Constructional Steel*
568 *Research*. 151 (2018) 146–173.
- 569 [43] Q. Yu, Z. Tao, Y.-X. Wu, Experimental behaviour of high performance concrete-filled steel
570 tubular columns, *Thin-Walled Structures*. 46 (2008) 362–370.